Characterization of the pairwise correlations in different quantum networks consisting of four-wave mixers and beamsplitters*

Jian Qi(祁健)[1], Jun Xin(忻俊)[1], Hai-Long Wang(王海龙)[1,†], and Jie-Tai Jing(荆杰泰)[1,2,‡]

[1] *State Key Laboratory of Precision Spectroscopy, School of Physics and Materials Science, East China Normal University, Shanghai* 200062, *China*

[2] *Collaborative Innovation Center of Extreme Optics, Shanxi University, Taiyuan* 030006, *China*

(Received 5 December 2016; revised manuscript received 3 March 2017; published online 6 June 2017)

We investigate the performances of the pairwise correlations (PCs) in different quantum networks consisting of four-wave mixers (FWMs) and beamsplitters (BSs). PCs with quantum correlation in different quantum networks can be verified by calculating the degree of relative intensity squeezing for any pair of all the output fields. More interestingly, the quantum correlation recovery and enhancement are present in the FWM+BS network and the repulsion effect phenomena (signal (idler)–frequency mode cannot be quantum correlated with the other two idler (signal)–frequency modes simultaneously) between the PCs with quantum correlation are predicted in the FWM + FWM and FWM + FWM + FWM networks. Our results presented here pave the way for the manipulation of the quantum correlation in quantum networks.

Keywords: pairwise correlation, four-wave mixer, degree of relative intensity squeezing, quantum network

PACS: 42.65.–k, 34.80.Pa, 03.65.Ud **DOI:** 10.1088/1674-1056/26/7/074214

1. Introduction

Quantum correlations shared between the multiple quantum correlated beams are the fundamental ingredients of the most continuous-variable (CV) quantum technologies.[1,2] The pairwise correlations (PCs) involved in the multiple quantum correlated beams are an important research subject. For example, Refs. [3], [4] and Ref. [5] gave the classification of three-qubit correlation and four-qubit correlation respectively, which both involve the consideration of PCs. Therefore, the quantum correlation shared by any pair of the multiple quantum correlated beams is worth studying. In recent years, four-wave mixers (FWMs) based on a hot rubidium vapor[6–21] have been proved to be very successful for many practical implementations, for example, tunable delay of Einstein–Podolsky–Rosen entangled states,[9] low-noise amplification of entangled states,[10] quantum mutual information,[13] and SU(1,1) interferometer[22,23] have been experimentally realized. In 2014, our group has experimentally realized the quantum correlated triple beams by cascading two FWM processes (FWM + FWM network) and strong relative intensity squeezing has been observed between the generated triple beams.[24] Reference [25] presents a scheme to realize the versatile quantum networks by cascading several FWM processes in warm rubidium vapors, and Refs. [26] and [27] discuss the tripartite entanglement and correlation in the cascaded FWM processes, but the PCs with quantum correlation are not compared between the FWM + FWM network and the FWM+beamsplitter (BS) network, let alone the quantum correlation recovery and enhancement of the PCs. However, in this paper, it can be found that the PCs with quantum correlation can be enhanced compared with the one of the single FWM process in the FWM+BS network. Therefore, we study the PCs[28–30] in different quantum networks, such as FWM + FWM, FWM+BS, FWM + FWM + FWM, and FWM + BS + BS networks. In addition, the repulsion effect phenomena between the PCs with quantum correlation are present in the FWM + FWM and FWM + FWM + FWM networks instead of the FWM+BS and FWM+BS+BS networks. This gives the prediction that signal (idler)–frequency mode cannot be quantum correlated with the other two idler (signal)–frequency modes simultaneously.

This article is organized as follows. In Section 2, we describe the quantum correlation performance of the FWM (BS) network using the degree of relative intensity squeezing (*DS*) criterion. In Section 3, we use the *DS* criterion to analyze the PCs existing in the FWM + FWM and FWM+BS networks. In Section 4, we analyze the PCs existing in the

*Project supported by the National Natural Science Foundation of China (Grants Nos. 91436211, 11374104, and 10974057), the Natural Science Foundation of Shanghai, China (Grant No. 17ZR1442900), the Specialized Research Fund for the Doctoral Program of Higher Education, China (Grant No. 20130076110011), the Program for Professor of Special Appointment (Eastern Scholar) at Shanghai Institutions of Higher Learning, the Program for New Century Excellent Talents in University, China (Grant No. NCET-10-0383), the Shu Guang Project supported by Shanghai Municipal Education Commission and Shanghai Education Development Foundation, China (Grant No. 11SG26), the Shanghai Pujiang Program, China (Grant No. 09PJ1404400), the Scientific Research Foundation for the Returned Overseas Chinese Scholars, State Education Ministry, National Basic Research Program of China (Grant No. 2016YFA0302103), and the Program of State Key Laboratory of Advanced 207 Optical Communication Systems and Networks, China (Grant No. 2016GZKF0JT003).

†Corresponding author. E-mail: wanghai55667788@126.com

‡Corresponding author. E-mail: jtjing@phy.ecnu.edu.cn

© 2017 Chinese Physical Society and IOP Publishing Ltd

FWM + FWM + FWM and FWM+BS+BS networks. In Section 5, we give a brief summary of this paper.

2. FWM (BS) network

In this section, we give a simple description of the FWM (BS) network. Firstly, we will focus on the FWM network. FWM is a nonlinear process which converts two pump photons into a probe photon and an idler photon. In the cell$_1$ of Fig. 1(a), an intense pump beam and a much weaker signal beam ($\hat{a}_0$) are crossed in the center of the rubidium vapor with a slight angle. Then the signal beam is amplified as $\hat{a}_2$ and a new beam called idler beam is generated as $\hat{a}_1$ on the other side of the pump beam at the same time. The signal beam and idler beam have different frequencies. The input–output relation of the FWM process shown in Fig. 1(a) is given by

$$\hat{a}_1 = \sqrt{G_1}\hat{a}_{v1} + \sqrt{g_1}\hat{a}_0^\dagger, \hat{a}_2 = \sqrt{G_1}\hat{a}_0 + \sqrt{g_1}\hat{a}_{v1}^\dagger, \quad (1)$$

where G_1 is the power gain in the FWM process and G_1-$g_1 = 1$, $\hat{a}_0$ is the coherent input signal and $\hat{a}_{v1}$ is the vacuum input, $\hat{a}_2$ is the amplified signal beam and $\hat{a}_1$ is the generated idler beam. See Ref. [6] for details. The relative intensity fluctuations $\mathrm{Var}(N_2 - N_1)_{\mathrm{FWM}}$ can be given by

$$\mathrm{Var}(N_2 - N_1)_{\mathrm{FWM}} = \langle \hat{a}_0^\dagger \hat{a}_0 \rangle, \quad (2)$$

where $\mathrm{Var}(A) = \langle A^2 \rangle - \langle A \rangle^2$ denotes the variance of A. The standard quantum limit (SQL) for the twin beams can be given by

$$\mathrm{Var}(N_2 - N_1)_{\mathrm{SQL}} = (2G_1 - 1)\langle \hat{a}_0^\dagger \hat{a}_0 \rangle. \quad (3)$$

The PC with quantum correlation between the twin beams $\hat{a}_1$ and $\hat{a}_2$ can be quantified using DS criterion, which is the ratio of the variance of the relative intensity for the twin beams to the variance at the SQL, namely

$$DS_{12}^{\mathrm{I}} = \frac{1}{2G_1 - 1}, \quad (4)$$

where the superscript and subscript for the DS_{ij}^k represent the network (we have three networks throughout the whole discussion, i.e., FWM (BS) network: 1 ($\widetilde{1}$), FWM + FWM (BS) network: 2 ($\widetilde{2}$), FWM + FWM (BS)+FWM (BS) network, 3 ($\widetilde{3}$)), the ith ($i = 1, 2, 3$) beam, and the jth ($j = 2, 3, 4$) beam in the network. The PC with quantum correlation of the twin beams from the FWM process can be demonstrated when $DS_{12}^{\mathrm{I}} < 1$ and can be easily obtained in the experiment since G_1 is always larger than 1. However, the values of DS of the individual beams $\hat{a}_1$ and $\hat{a}_2$ are given by

$$DS_1^{\mathrm{I}} = DS_2^{\mathrm{I}} = 2G_1 - 1. \quad (5)$$

This corresponds to a linear increase in the noise on both the signal and idler beams as gain is increased. Thus the twin beams $\hat{a}_1$ and $\hat{a}_2$ in the FWM process are both in thermal states. Equations (4) and (5) demonstrate that the PC with quantum correlation for the twin beams is present at the expense of increasing the fluctuations in the individual beams when $G_1 > 1$.

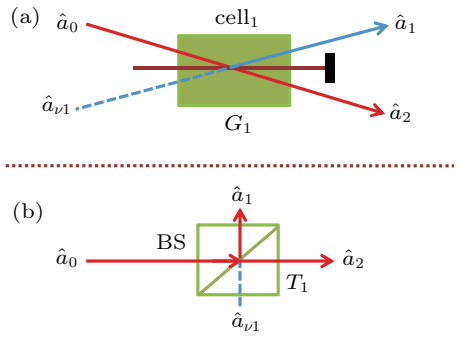


Fig. 1. (color online) FWM (BS) network. (a) FWM network. $\hat{a}_0$ is the coherent input signal and $\hat{a}_{v1}$ is the vacuum input. $\hat{a}_2$ is the amplified signal beam and $\hat{a}_1$ is the generated idler beam. G_1 is the power gain of the FWM process. (b) BS network. $\hat{a}_0$ is the coherent input signal and $\hat{a}_{v1}$ is the vacuum input. $\hat{a}_1$ and $\hat{a}_2$ are two output beams. T_1 is the transmission of the BS.

Secondly, for the BS network in Fig. 1(b), the input–output relationship can be given by

$$\hat{a}_1 = \sqrt{T_1}\hat{a}_{v1} - \sqrt{1 - T_1}\hat{a}_0,$$
$$\hat{a}_2 = \sqrt{T_1}\hat{a}_0 + \sqrt{1 - T_1}\hat{a}_{v1}, \quad (6)$$

where T_1 is the transmission of the BS. $\hat{a}_0$ is the coherent input signal and $\hat{a}_{v1}$ is the vacuum input. The values of DS of the individual beams $\hat{a}_1$ and $\hat{a}_2$ are given by

$$DS_1^{\widetilde{\mathrm{I}}} = DS_2^{\widetilde{\mathrm{I}}} = 1. \quad (7)$$

The DS between the beams $\hat{a}_1$ and $\hat{a}_2$ can be given by

$$DS_{12}^{\widetilde{\mathrm{I}}} = 1. \quad (8)$$

As we can see from Eq. (8), the DS between the beams $\hat{a}_1$ and $\hat{a}_2$ is independent of the transmission of the BS, thus equation (8) represents the correlation level between the two beams in both the coherent states or one beam in the coherent state, the other in the vacuum state. Equations (4) and (8) demonstrate that the PC with quantum correlation cannot be obtained by BS with a coherent state and a vacuum state inputs due to its passive nature and the FWM process with G_1=1 is equivalent to the BS with $T_1 = 1$.

3. FWM + FWM (BS) network

In this section, we analyze the network in which one of the twin beams is amplified or attenuated by one FWM or BS, respectively. Here the FWM and BS can be considered as the gain beamsplitter[21] or lossy beamsplitter, respectively. Firstly, we will focus on the FWM + FWM network. We take the signal beam from the first FWM process (cell$_1$) as the seed for the second FWM process (cell$_2$) in Fig. 2(a).[24] $\hat{a}_1$, $\hat{a}_2$, and

$\hat{a}_3$ are the triple newly-generated beams in the output stage of the FWM + FWM network. In our previous work,[24] we have shown the generation of strong quantum correlation between the triple bright beams but not the PCs with quantum correlation for any pair of the triple beams. Here we will study all the possible PCs of the triple beams $\hat{a}_1$, $\hat{a}_2$, and $\hat{a}_3$ in Fig. 2(a). The input–output relationship of the FWM + FWM network in Fig. 2(a) can be written as

$$\begin{aligned}
N_1 &= (G_1-1)(N_0+1)+\sqrt{G_1(G_1-1)}(\hat{a}_0\hat{a}_{v1}+\hat{a}_0^{\dagger}\hat{a}_{v1}^{\dagger}),\\
N_2 &= G_1G_2N_0+G_2\sqrt{G_1(G_1-1)}(\hat{a}_0\hat{a}_{v1}+\hat{a}_0^{\dagger}\hat{a}_{v1}^{\dagger})\\
&\quad+\sqrt{G_1G_2(G_2-1)}(\hat{a}_0\hat{a}_{v2}+\hat{a}_0^{+}\hat{a}_{v2}^{\dagger}),\\
N_3 &= G_1(G_2-1)(N_0+1)+(G_2-1)\\
&\quad\times\sqrt{G_1(G_1-1)}(\hat{a}_0\hat{a}_{v1}+\hat{a}_0^{\dagger}\hat{a}_{v1}^{\dagger})\\
&\quad+\sqrt{G_1G_2(G_2-1)}(\hat{a}_0\hat{a}_{v2}+\hat{a}_0^{\dagger}\hat{a}_{v2}^{\dagger}), \qquad (9)\\
\hat{a}_1 &= \sqrt{G_1}\hat{a}_{v1}+\sqrt{g_1}\hat{a}_0^{\dagger},\\
\hat{a}_2 &= \sqrt{G_1G_2}\hat{a}_0+\sqrt{G_2g_1}\hat{a}_{v1}^{\dagger}+\sqrt{g_2}\hat{a}_{v2}^{\dagger},\\
\hat{a}_3 &= \sqrt{G_2}\hat{a}_{v2}+\sqrt{G_1g_2}\hat{a}_0^{\dagger}+\sqrt{g_1g_2}\hat{a}_{v1}, \qquad (10)
\end{aligned}$$

where G_1 and G_2 are the power gains for the cell$_1$ and cell$_2$, respectively. It should be noted that the DS of the triple beams ($\hat{a}_1$, $\hat{a}_2$, and $\hat{a}_3$) is given by

$$DS_{123}^2=\frac{\mathrm{Var}(N_2-N_1-N_3)_{\mathrm{FWM}}}{\mathrm{Var}(N_2-N_1-N_3)_{\mathrm{SQL}}}=\frac{1}{2G_1G_2-1}. \qquad (11)$$

Compared to Eq. (4), equation (11) means that the FWM + FWM network can enhance the quantum correlation of the system. The quantum correlation shared by the triple beams is present if $G_1G_2>1$, i.e., $G_1>1$ or $G_2>1$.

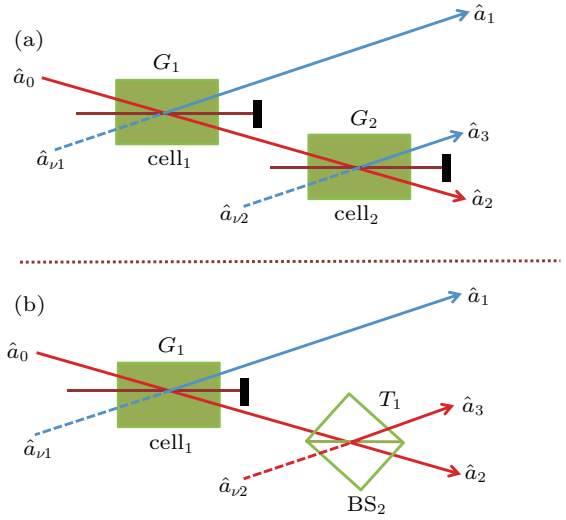


Fig. 2. (color online) FWM + FWM (BS) network. (a) FWM + FWM network. $\hat{a}_0$ is coherent input signal. $\hat{a}_{v1}$ and $\hat{a}_{v2}$ are vacuum inputs. G_1 and G_2 are the power gains of cell$_1$ and cell$_2$, respectively. $\hat{a}_1$, $\hat{a}_2$, and $\hat{a}_3$ are the triple output beams. (b) FWM+BS network. $\hat{a}_0$ is coherent input signal. $\hat{a}_{v1}$ and $\hat{a}_{v2}$ are vacuum inputs. G_1 is the power gain of cell$_1$. T_1 is the transmission of the BS. $\hat{a}_1$, $\hat{a}_2$, and $\hat{a}_3$ are the triple output beams.

PC between $\hat{a}_1$ and $\hat{a}_2$ can be quantified by

$$DS_{12}^2=\frac{2G_1^2G_2^2-4G_1^2G_2+2G_1^2+3G_1G_2-3G_1+1}{G_1G_2+G_1-1}. \qquad (12)$$

Equation (12) will be reduced to $2G_2-1$ and $1/(2G_1-1)$ when we set G_1=1 and G_2=1 respectively, corresponding to the cases of Eq. (5) and Eq. (4) respectively. The physical meaning is as follows. When we set G_1=1, the PC between the thermal states $\hat{a}_1$ and $\hat{a}_2$ translates into the one between the vacuum state $\hat{a}_1$ and the thermal state $\hat{a}_2$, i.e., $DS_{12}^2=2G_2-1$. When we set $G_2=1$, the PC between the thermal states $\hat{a}_1$ and $\hat{a}_2$ translates into the one between the twin beams from the first FWM process, i.e., $DS_{12}^2=1/(2G_1-1)$. The region in which $DS_{12}^2<1$, i.e., there exists quantum correlation between the beams $\hat{a}_1$ and $\hat{a}_2$, is shown in purple denoted as (1, 2) in Fig. 3. The value of G_2 on the boundary (see the boundary given by $G_2=1+(\sqrt{4G_1-3}-1)/2G_1$ in Fig. 3) of that region reaches its maximal value of 1.33 when $G_1=3$, and it decreases when $G_1>3$ and will eventually reach the value of 1. The study of DS_{12}^2 presented above is actually the question of how to preserve or even enhance the quantum correlation between the beams $\hat{a}_1$ and $\hat{a}_2$ compared with the one between the twin beams from the first FWM process under the introduction of a gain beamsplitter which brings the deterioration effect to the quantum correlation by the quantum amplification of one of the beams ($\hat{a}_2$). The results shown in Fig. 3 actually show the value of G_2 on the boundary below which the quantum correlation can always be preserved as the value of G_1 increases. More interestingly, in this network, the PC with quantum correlation between the beams $\hat{a}_1$ and $\hat{a}_2$ cannot be quantum recovered to the one between the twin beams from the first FWM process, i.e., $DS_{12}^2>DS_{12}^1$ for any value of G_1, $G_2>1$ due to the quantum amplification from the gain beamsplitter. The condition of $DS_{12}^2=DS_{12}^1$ is given by $G_2=2(G_1-1)^2/G_1(2G_1-1)$ as shown in the inset of Fig. 3. With the increasing of G_1, the value of G_2 always increases and eventually saturates at the value of 1, but $G_2>1$ is required for the generation of the triple quantum correlated beams. That is to say, quantum amplification of the signal beam of the twin beams can destroy the quantum correlation between the twin beams inevitably.

PC between $\hat{a}_1$ and $\hat{a}_3$ can be quantified by

$$DS_{13}^2=\frac{2G_1^2G_2^2-8G_1^2G_2+8G_1^2+5G_1G_2-8G_1+1}{G_1G_2-1}. \qquad (13)$$

Equation (13) is equal to 1 when $G_2=2-1/G_1$. Except that, DS_{13}^2 is always larger than 1, i.e., there is no quantum correlation between the beams $\hat{a}_1$ and $\hat{a}_3$. The region in which $DS_{13}^2=1$ ($G_2=2-1/G_1$) is shown as the red line denoted as (1, 3) in Fig. 3. In this sense, there is no quantum correlation between the beams $\hat{a}_1$ and $\hat{a}_3$ for any value of G_1 and G_2 since DS_{13}^2 is always more than or equal to 1.

PC between $\hat{a}_2$ and $\hat{a}_3$ can be quantified by

$$DS^2_{23} = \frac{2G_1 - 1}{2G_2 - 1}. \tag{14}$$

The region in which $DS^2_{23} < 1$ ($G_1 < G_2$) is shown in cyan denoted as (2, 3) in Fig. 3. Therefore, the PC with quantum correlation between the beams $\hat{a}_2$ and $\hat{a}_3$ will be present for any $G_1 < G_2$. This is not difficult to figure out if one looks at the functional form of Eq. (14). In the region $G_1 < G_2$, the existence of quantum correlation between the beams $\hat{a}_2$ and $\hat{a}_3$ eliminates the possibility of the one between the beams $\hat{a}_2$ and $\hat{a}_1$. In other words, beam $\hat{a}_2$ cannot be quantum correlated with beams $\hat{a}_1$ and $\hat{a}_3$ in the same gain region. In this sense, we could call this phenomena repulsion effect of quantum correlation between the PCs in the FWM + FWM network.

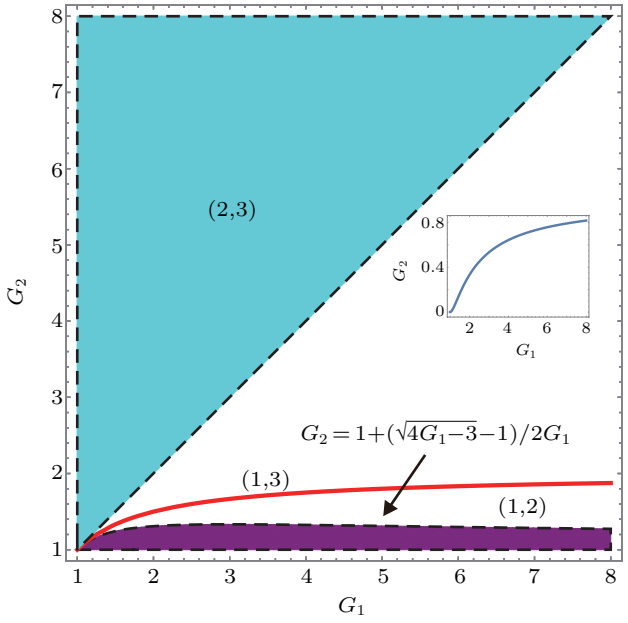


Fig. 3. (color online) The region plot of Eqs. (12)–(14). The purple region (1, 2) is the region of $DS^2_{12} < 1$, the red line (1, 3) is the region of $DS^2_{13} = 1$ ($G_2 = 2 - 1/G_1$), and the cyan region (2, 3) is the region of $DS^2_{23} < 1$. Inset: $G_2 = 2(G_1 - 1)^2/G_1(2G_1 - 1)$.

Secondly, for the FWM+BS network in Fig. 2(b), the DS of the triple beams is given by

$$DS^2_{123} = \frac{\mathrm{Var}(N_1 - N_2 - N_3)_{\mathrm{FWM}}}{\mathrm{Var}(N_1 - N_2 - N_3)_{\mathrm{SQL}}} = \frac{1}{2G_1 - 1}. \tag{15}$$

Compared to Eq. (11), this network cannot enhance the quantum correlation existing in the triple beams $\hat{a}_1$, $\hat{a}_2$, and $\hat{a}_3$ in Fig. 2(b). We will also analyze all the possible PCs.

PC between $\hat{a}_1$ and $\hat{a}_2$ can be quantified by

$$DS^2_{12} = 1 + \frac{2(G_1 - 1)(G_1(T_1 - 1)^2 - 1)}{G_1 T_1 + G_1 - 1}. \tag{16}$$

Equation (16) will be reduced to $1/(2G_1 - 1)$, $2G_1 - 1$, and 1 when we set T_1=1, T_1=0, and G_1=1 respectively, corresponding to the cases of Eq. (4), Eq. (5), and Eq. (8) respectively. These phenomena can be understood as follows. When we set T_1=1, the PC between the thermal states $\hat{a}_1$ and $\hat{a}_2$ translates into the one between the twin beams from the first FWM process, i.e., $DS^2_{12} = 1/(2G_1 - 1)$. When we set $T_1 = 0$, the PC between the thermal states $\hat{a}_1$ and $\hat{a}_2$ translates into the one between the thermal state $\hat{a}_1$ and the vacuum state $\hat{a}_2$, i.e., $DS^2_{12} = 2G_1 - 1$. When we set $G_1 = 1$, the PC between the thermal states $\hat{a}_1$ and $\hat{a}_2$ translates into the one between the vacuum state $\hat{a}_1$ and the coherent state $\hat{a}_2$, i.e., $DS^2_{12} = 1$. This theoretical result is consistent with Eq. (5) in Ref. [31]. The region in which $DS^2_{12} < 1$, i.e., there exists quantum correlation between the beams $\hat{a}_1$ and $\hat{a}_2$, is shown in green denoted as (1, 2) in Fig. 4(a). Different from the boundary of the DS^2_{12}, with the increasing of G_1, the value of T_1 on the boundary always increases and eventually saturates at the value of 1 (see the boundary given by $T_1 = 1 - 1/\sqrt{G_1}$ in Fig. 4(a)). The study of DS^2_{12} presented above is actually the question of how to preserve or even enhance the quantum correlation between the beams $\hat{a}_1$ and $\hat{a}_2$ compared with the one between the twin beams under the introduction of a lossy beamsplitter which brings the deterioration effect to the quantum correlation by the attenuation of one of the beams ($\hat{a}_2$). The results shown in Fig. 4(a) actually show the value of T_1 on the boundary above which the quantum correlation can always be preserved as the value of G_1 increases. More interestingly, in this case, the PC with quantum correlation between the beams $\hat{a}_1$ and $\hat{a}_2$ can be quantum recovered and enhanced compared with the one between the twin beams from the first FWM process, i.e., $DS^2_{12} \leq DS^1_{12}$, when $T_1 \geq 2(G_1 - 1)/(2G_1 - 1)$. The results shown in Fig. 4(a) actually shows the boundary (the red line in Fig. 4(a)) for the values of T_1 above which the quantum correlation enhancement can always be realized as the value of G_1 increases. That is to say, certain attenuation of the signal beam of the twin beams can recover and enhance the quantum correlation between the twin beams from the first FWM process.

PC between $\hat{a}_1$ and $\hat{a}_3$ can be quantified by

$$DS^2_{13} = \frac{1 - G_1 T_1 - 2G_1 T_1^2 + 2G_1^2 T_1^2}{(G_1 - 1) + G_1(1 - T_1)}. \tag{17}$$

The region in which $DS^2_{13} < 1$, i.e., there exists quantum correlation between the beams $\hat{a}_1$ and $\hat{a}_3$, is shown in magenta denoted as (1, 3) in Fig. 4(b). With the increasing of G_1, the value of T_1 on the boundary always decreases and eventually reaches the value of 0 (see the boundary given by $T_1 = 1/\sqrt{G_1}$ in Fig. 4(b)). As shown in Fig. 4, the sum of the boundary value of the DS^2_{12}, i.e., $T_1 = 1 - 1/\sqrt{G_1}$, and the boundary value of DS^2_{13}, i.e., $T_1 = 1/\sqrt{G_1}$, is always equal to 1. That is to say, the PCs with quantum correlation between DS^2_{12} and DS^2_{13} is limited by the lossy beamsplitter. In addition, the crossing region of $DS^2_{12} < 1$ and $DS^2_{13} < 1$ is present in Figs. 4(a) and

4(b), which means that the repulsion effect is absent for the FWM+BS network.

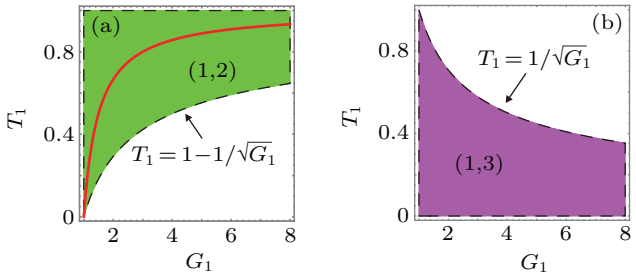


Fig. 4. (color online) The region plot of Eqs. (16) and (17). (a) The green region (1, 2) is the region of $DS^2_{12}<1$ and the red line is $T_1=2(G_1-1)/(2G_1-1)$. (b) The magenta region (1, 3) is the region of $DS^2_{13}<1$.

PC between $\hat{a}_2$ and $\hat{a}_3$ can be quantified by

$$DS^2_{23}=(2T_1-1)^2(2G_1-1)+4T_1(1-T_1), \tag{18}$$

which is equal to 1 when G_1=1 or T_1=1/2. As we all know, in order to generate the SQL, the shot noise limited beam, such as coherent state beam, is always preferred as shown in Eq. (8). $T_1=1/2$ means that the balanced differential measurement of a thermal state can also obtain the SQL. Except that, DS^2_{23} is always larger than 1, i.e., there is no quantum correlation between the beams $\hat{a}_2$ and $\hat{a}_3$ for any value of G_1 and T_1, since DS^2_{23} is always more than or equal to 1.

As Section 3 mentioned, the FWM (gain beamsplitter) will inevitably destroy the quantum correlation between the twin beams $\hat{a}_1$ and $\hat{a}_2$ from the first FWM process, while BS (lossy beamsplitter) can preserve or even enhance the quantum correlation between the twin beams $\hat{a}_1$ and $\hat{a}_2$. The repulsion effect between the PCs with quantum correlation is predicted in the gain beamsplitter case (FWM + FWM network) instead of the lossy beamsplitter case (FWM+BS network).

4. FWM + FWM (BS)+FWM (BS) network

In this section, we analyze the network in which both of the twin beams are amplified or attenuated by two FWMs or BSs respectively. Here the FWM and BS can also be considered as the gain beamsplitter and lossy beamsplitter, respectively. Firstly, we will focus on the FWM + FWM + FWM network. We take the signal beam from the first FWM process (cell_1) as the seed for the second FWM (cell_2) and the idler beam as the seed for the third FWM (cell_3) in Fig. 5(a). $\hat{a}_1$, $\hat{a}_2$, $\hat{a}_3$, and $\hat{a}_4$ are the quadruple newly-generated beams in the output stage of the FWM + FWM + FWM network. The input–output relationship of the FWM + FWM + FWM network in Fig. 5(a) can be written as

$$\begin{aligned}\hat{a}_1 &= \sqrt{G_1G_2}\hat{a}_{v1}+\sqrt{G_2g_1}\hat{a}_0^\dagger+\sqrt{g_2}\hat{a}_{v3}^\dagger,\\ \hat{a}_2 &= \sqrt{G_1G_2}\hat{a}_0+\sqrt{G_2g_1}\hat{a}_{v1}^\dagger+\sqrt{g_2}\hat{a}_{v2}^\dagger,\\ \hat{a}_3 &= \sqrt{G_2}\hat{a}_{v2}+\sqrt{G_1g_2}\hat{a}_0^\dagger+\sqrt{g_1g_2}\hat{a}_{v1},\\ \hat{a}_4 &= \sqrt{G_2}\hat{a}_{v3}+\sqrt{G_1g_2}\hat{a}_{v1}^\dagger+\sqrt{g_1g_2}\hat{a}_0,\end{aligned} \tag{19}$$

where G_1 is the power gain of cell_1 and G_2 is the power gain of the cell_2 and cell_3. It should be noted the *DS* of the quadruple beams ($\hat{a}_1$, $\hat{a}_2$, $\hat{a}_3$, and $\hat{a}_4$) is given by

$$\begin{aligned}DS^3_{1234} &= \frac{\text{Var}(N_1-N_4-N_2+N_3)_{\text{FWM}}}{\text{Var}(N_1-N_4-N_2+N_3)_{\text{SQL}}}\\ &= \frac{1}{(2G_1-1)(2G_2-1)}.\end{aligned} \tag{20}$$

Compared to Eq. (11), this network has also enhanced the quantum correlation of the system. The quantum correlation shared by the quadruple beams is present if $(2G_1-1)(2G_2-1)>1$, i.e., $G_1>1$ or $G_2>1$. Next let us analyze all the possible PCs in this network.

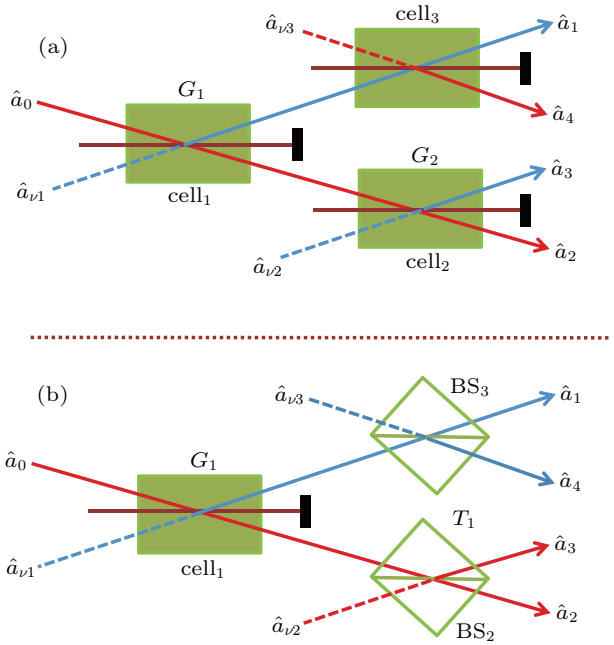


Fig. 5. (color online) FWM + FWM (BS)+FWM (BS) network. (a) FWM + FWM + FWM network. $\hat{a}_0$ is coherent input signal. $\hat{a}_{v1}$, $\hat{a}_{v2}$, and $\hat{a}_{v3}$ are vacuum inputs. G_1 is the power gain of the cell_1. Cell_2 and cell_3 have the same power gains G_2 for simplicity. $\hat{a}_1$, $\hat{a}_2$, $\hat{a}_3$, and $\hat{a}_4$ are the quadruple output beams. (b) FWM+BS+BS network. $\hat{a}_0$ is coherent input signal. $\hat{a}_{v1}$, $\hat{a}_{v2}$, and $\hat{a}_{v3}$ are vacuum inputs. G_1 is the power gain of the cell_1. BS_2 and BS_3 have the same transmissions T_1 for simplicity. $\hat{a}_1$, $\hat{a}_2$, $\hat{a}_3$, and $\hat{a}_4$ are the quadruple output beams.

PC between $\hat{a}_1$ and $\hat{a}_2$ can be quantified by

$$DS^3_{12}=\frac{2G_1G_2-2G_1+1}{2G_1-1}. \tag{21}$$

Equation (21) will be reduced to $2G_2-1$ and $1/(2G_1-1)$ when we set $G_1=1$ and $G_2=1$ respectively, similar to the case of Eq. (12). The region in which $DS^3_{12}<1$ is shown in purple denoted as (1, 2) in Fig. 6. With the increasing of G_1, the value of G_2 on the boundary always increases and eventually saturates at the value of 2 (see the boundary given by $G_2=2-1/G_1$ in Fig. 6). The study of DS^3_{12} presented above is actually the question of how to preserve or even enhance the

quantum correlation between the beams $\hat{a}_1$ and $\hat{a}_2$ under the introduction of two gain beamsplitters which bring the deterioration effect to the quantum correlation by the quantum amplification of both of the beams ($\hat{a}_1$ and $\hat{a}_2$). The results shown in Fig. 6 actually show the boundary for the values of G_2 below which the quantum correlation can always be preserved as the value of G_1 increases. More interestingly, in this case, the PC with quantum correlation between the beams $\hat{a}_1$ and $\hat{a}_2$ can be quantum recovered to the one between the twin beams from the first FWM process only when $G_2 = 1$ (the inset of Fig. 6), i.e., $DS^3_{12} = DS^1_{12}$. But it means that the generation of the quadruple quantum correlated beams is impossible due to the absence of the cell$_2$ and cell$_3$. That is to say, the quantum correlation recovery and enhancement are impossible for the FWM + FWM + FWM network.

PC between $\hat{a}_1$ and $\hat{a}_3$ ($\hat{a}_2$ and $\hat{a}_4$) can be quantified by

$$\begin{aligned} DS^3_{13} &= \frac{-4G_1G_2 + 2G_1G_2^2 + 2G_1^2 - G_1 + G_2}{2G_1G_2 - G_1 - G_2} \\ DS^3_{24} &= \frac{2G_1G_2^2 + 2G_1^2 - 3G_1 - G_2 + 1}{2G_1G_2 - G_1 - G_2 + 1}. \end{aligned} \tag{22}$$

Equation (23) is always larger than 1 for any value of G_1 and G_2. In this sense, there is no quantum correlation between the beams $\hat{a}_1$ and $\hat{a}_3$ ($\hat{a}_2$ and $\hat{a}_4$), since DS^3_{13} (DS^3_{24}) is always larger than 1 for any value of G_1 and G_2.

PC between $\hat{a}_1$ and $\hat{a}_4$ ($\hat{a}_2$ and $\hat{a}_3$) can be quantified by

$$DS^3_{14} = \frac{2G_1 - 1}{2G_2 - 1}\left(DS^3_{23} = \frac{2G_1 - 1}{2G_2 - 1}\right). \tag{23}$$

Equation (22) is similar to the case of Eq. (14). The region in which $DS^3_{14} < 1$ ($DS^3_{23} < 1$) is shown in cyan denoted as ((1, 4), (2, 3)) in Fig. 6. Therefore, beams $\hat{a}_1$ ($\hat{a}_2$) and $\hat{a}_4$ ($\hat{a}_3$) are quantum correlated within the cyan region ($G_1 < G_2$) in Fig. 6.

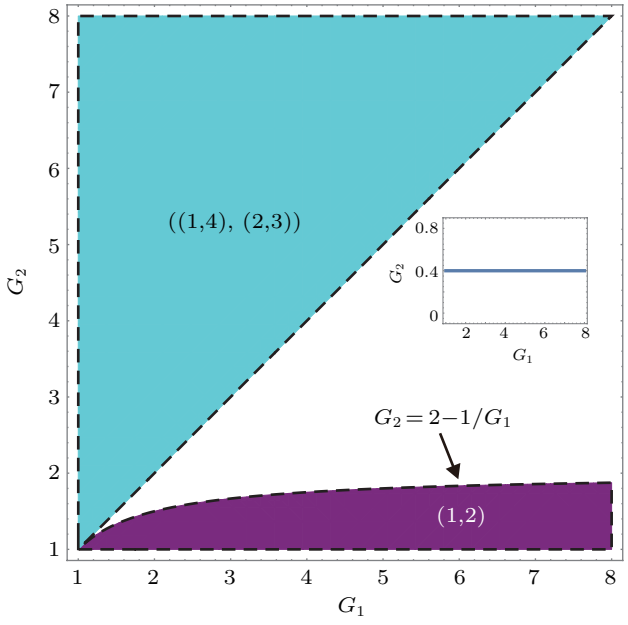


Fig. 6. (color online) The region plot of Eqs. (21) and (23). The purple region (1, 2) is the region of $DS^3_{12} < 1$ and the cyan region ((1, 4), (2, 3)) is the region of $DS^3_{14} < 1$ and $DS^3_{23} < 1$. Inset: $G_2 = 1$.

PC between $\hat{a}_3$ and $\hat{a}_4$ can be quantified by

$$DS^3_{34} = \frac{2G_1G_2 - 1}{2G_1 - 1}. \tag{24}$$

The PC with quantum correlation between the beams $\hat{a}_3$ and $\hat{a}_4$ will be absent because G_2 is always more than or equal to 1. This can be easily understood if one looks at the functional form of Eq. (24). As discussed above, for this FWM + FWM + FWM network, there are three possible PCs with quantum correlation, namely DS^3_{12}, DS^3_{14}, and DS^3_{23}. In addition, the existence of quantum correlation between the beams $\hat{a}_1$ and $\hat{a}_2$ eliminates the possibility of the one between the beams $\hat{a}_1$ ($\hat{a}_3$) and $\hat{a}_4$ ($\hat{a}_2$). In other words, beam $\hat{a}_1$ ($\hat{a}_2$) cannot be quantum correlated with the beams $\hat{a}_2$ ($\hat{a}_1$) and $\hat{a}_4$ ($\hat{a}_3$) in the same gain region. These effects in this FWM + FWM + FWM network are similar to the above mentioned repulsion effect of quantum correlation between the PCs in the FWM + FWM network.

Secondly, for the FWM+BS+BS network in Fig. 5(b), the DS of the quadruple beams is given by

$$DS^{\tilde{3}}_{1234} = \frac{\mathrm{Var}(N_1 + N_4 - N_2 - N_3)_{\mathrm{FWM}}}{\mathrm{Var}(N_1 + N_4 - N_2 - N_3)_{\mathrm{SQL}}} = \frac{1}{(2G_1 - 1)}. \tag{25}$$

In this case, the quantum correlations for the quadruple beams have remained unchanged compared with the Eq. (4). We will analyze all the possible PCs.

PC between $\hat{a}_1$ and $\hat{a}_2$ can be quantified by

$$DS^{\tilde{3}}_{12} = 1 - T_1 + \frac{T_1}{2G_1 - 1}. \tag{26}$$

Equation (26) will be reduced to 1, $1/(2G_1 - 1)$, and 1 when we set $G_1 = 1$, $T_1 = 1$, and $T_1 = 0$ respectively, corresponding to the cases of Eq. (8), Eq. (4), and Eq. (8) respectively. We can understand these physical phenomena as follows. When we set G_1=1, the PC between the thermal states $\hat{a}_1$ and $\hat{a}_2$ translates into the one between the vacuum state $\hat{a}_1$ and the coherent state $\hat{a}_2$, i.e., $DS^{\tilde{3}}_{12} = 1$. When we set $T_1 = 1$, the PC between the thermal states $\hat{a}_1$ and $\hat{a}_2$ translates into the one between the twin beams from the first FWM process, i.e., $DS^{\tilde{3}}_{12} = 1/(2G_1 - 1)$. When we set $T_1 = 0$, the PC between the thermal states $\hat{a}_1$ and $\hat{a}_2$ translates into the one between the vacuum state $\hat{a}_1$ and the vacuum state $\hat{a}_2$, i.e., $DS^{\tilde{3}}_{12} = 1$. Its value is always less than or equal to 1 for any value of G_1 and T_1. The region in which $DS^{\tilde{3}}_{12} < 1$, i.e., there exists quantum correlation between the beams $\hat{a}_1$ and $\hat{a}_2$, is shown in Fig. 7(a). Figure 7(a) means the larger G_1 and larger T_1 are preferred for the PC with quantum correlation between the beams $\hat{a}_1$ and $\hat{a}_2$. The study of $DS^{\tilde{3}}_{12}$ presented above is actually the question of how to preserve or even enhance the quantum correlation between the beams $\hat{a}_1$ and $\hat{a}_2$ under the introduction of two lossy beamsplitters which bring the deterioration effect to the quantum correlation by the same amount of attenuation of

both of the beams ($\hat{a}_1$ and $\hat{a}_2$). Figure 7(a) shows that the same amount of attenuation can preserve the PC with quantum correlation between the beams $\hat{a}_1$ and $\hat{a}_2$. More interestingly, in this case, the PC with quantum correlation between the beams $\hat{a}_1$ and $\hat{a}_2$ can be quantum recovered to the one between the twin beams from the first FWM process only when $T_1 = 1$, i.e., $DS^{\tilde{3}}_{12} = DS^{1}_{12}$. That is to say, when $T_1 < 1$, both attenuation of the twin beams can destroy the quantum correlation between the twin beams from the first FWM process inevitably.

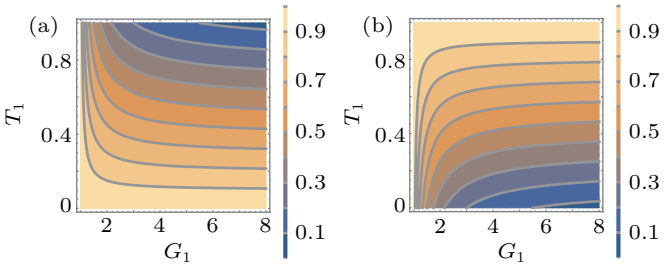


Fig. 7. (color online) The contour plot of Eqs. (26) and (30). (a) The contour plot of $DS^{\tilde{3}}_{12} < 1$. (b) The contour plot of $DS^{\tilde{3}}_{34} < 1$.

PC between $\hat{a}_1$ and $\hat{a}_3$ can be quantified by

$$DS^{\tilde{3}}_{13} = \frac{-G_1 + 2G_1^2 - T_1 + 8G_1T_1 - 8G_1^2T_1 + 2T_1^2 - 10G_1T_1^2 + 8G_1^2T_1^2}{G_1(1-T_1) + (G_1-1)T_1}. \tag{27}$$

The region in which $DS^{\tilde{3}}_{13} < 1$, i.e., there exists quantum correlation between the beams $\hat{a}_1$ and $\hat{a}_3$, is shown in magenta denoted as (1, 3) in Fig. 8(a). Figure 8(a) means that the PC with quantum correlation between the beams $\hat{a}_1$ and $\hat{a}_3$ is present for the value of T_1 between the two boundaries $T_1 = (2G_1 + \sqrt{G_1})/(4G_1 - 1)$ and $T_1 = (2G_1 - \sqrt{G_1})/(4G_1 - 1)$. With the increasing of G_1, the values of T_1 on the boundaries eventually reach the value of 1/2.

PC between $\hat{a}_1$ and $\hat{a}_4$ ($\hat{a}_2$ and $\hat{a}_3$) can be quantified by

$$\begin{aligned} DS^{\tilde{3}}_{14} &= (2T_1 - 1)^2(2G_1 - 1) + 4T_1(1 - T_1) \\ (DS^{\tilde{3}}_{23} &= (2T_1 - 1)^2(2G_1 - 1) + 4T_1(1 - T_1)), \end{aligned} \tag{28}$$

which is similar to the case of Eq. (18). Therefore, the beams $\hat{a}_1$ ($\hat{a}_2$) and $\hat{a}_4$ ($\hat{a}_3$) are not quantum correlated to each other in this network.

PC between $\hat{a}_2$ and $\hat{a}_4$ can be quantified by

$$DS^{\tilde{3}}_{24} = \frac{1 - 3G_1 + 2G_1^2 - 3T_1 + 12G_1T_1 - 8G_1^2T_1 + 2T_1^2 - 10G_1T_1^2 + 8G_1^2T_1^2}{G_1T_1 + (G_1 - 1)(1 - T_1)}. \tag{29}$$

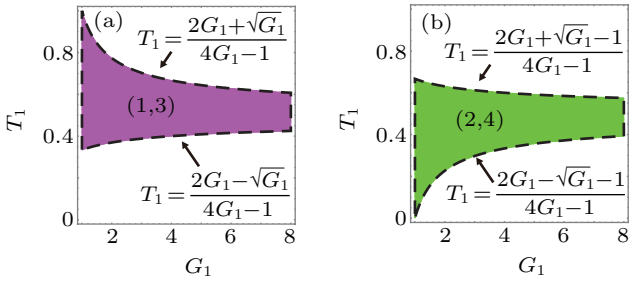


Fig. 8. (color online) The region plot of Eqs. (27) and (29). (a) The magenta region is the region of $DS^{\tilde{3}}_{13} < 1$. (b) The green region is the region of $DS^{\tilde{3}}_{24} < 1$.

The region in which $DS^{\tilde{3}}_{24} < 1$, i.e., there exists quantum correlation between the beams $\hat{a}_2$ and $\hat{a}_4$, is shown in green denoted as (2, 4) in Fig. 8(b). Figure 8(b) means that the PC with quantum correlation between the beams $\hat{a}_2$ and $\hat{a}_4$ is present for the value of T_1 between the two boundaries $T_1 = (2G_1 + \sqrt{G_1} - 1)/(4G_1 - 1)$ and $T_1 = (2G_1 - \sqrt{G_1} - 1)/(4G_1 - 1)$. With the increasing of G_1, the values of T_1 on the boundaries eventually reach the value of 1/2. As shown in Fig. 8, the sum of the boundary value of $DS^{\tilde{3}}_{13}$, i.e., $T_1 = (2G_1 + \sqrt{G_1})/(4G_1 - 1)$ ($T_1 = (2G_1 - \sqrt{G_1})/(4G_1 - 1)$), and the boundary value of $DS^{\tilde{3}}_{24}$, i.e., $T_1 = (2G_1 - \sqrt{G_1} - 1)/(4G_1 - 1)$ ($T_1 = (2G_1 + \sqrt{G_1} - 1)/(4G_1 - 1)$), is always equal to 1 due to the limitation of the lossy beamsplitter.

PC between $\hat{a}_3$ and $\hat{a}_4$ can be quantified by

$$DS^{\tilde{3}}_{34} = T_1 + \frac{(1 - T_1)}{2G_1 - 1}, \tag{30}$$

which is always less than or equal to 1 for any value of G_1 and T_1. The region in which $DS^{\tilde{3}}_{34} < 1$, i.e., there exists quantum correlation between the beams $\hat{a}_3$ and $\hat{a}_4$, is shown in Fig. 7(b). Figure 7(b) means that the larger G_1 and smaller T_1 are preferred for the PC with quantum correlation between $\hat{a}_3$ and $\hat{a}_4$.

As Section 4 mentioned, both the FWM + FWM + FWM and FWM+BS+BS networks can preserve the quantum correlation between $\hat{a}_1$ and $\hat{a}_2$ under the condition of $G_2 = 1$ and $T_1 = 1$, respectively. The repulsion effect between the PCs with quantum correlation is also predicted in the FWM + FWM + FWM network instead of the FWM+BS+BS network.

5. Conclusion

In summary, we theoretically characterize the performances of the PCs in different quantum networks consisting of FWMs and BSs. The quantum correlation recovery and enhancement are present in the FWM+BS network and the repulsion effect phenomena between the PCs with quantum correlation are predicted in the FWM + FWM and FWM + FWM + FWM networks. Our results presented here pave the way for the manipulation of the quantum correlation in quantum networks.

References

[1] Kimble H J 2008 *Nature* **453** 1023
[2] Braunstein S L and Loock P V 2005 *Rev. Mod. Phys.* **77** 513
[3] Borsten L, Dahanayake D, Duff M J, Rubens W and Ebrahim H 2008 *Phys. Rev. A* **80** 032326
[4] Acín A, Bruß D, Lewenstein A and Sanpera A 2001 *Phys. Rev. Lett.* **87** 040401
[5] Borsten L, Dahanayake D, Duff M J, Marrani A and Rubens W 2010 *Phys. Rev. Lett.* **105** 100507
[6] McCormcik C F, Boyer V, Arimondo E and Lett P D 2007 *Opt. Lett.* **32** 178
[7] Boyer V, Marino A M and Lett P D 2008 *Phys. Rev. Lett.* **100** 143601
[8] Boyer V, Marino A M, Pooser R C and Lett P D 2008 *Science* **321** 544
[9] Marino A M, Pooser R C, Boyer V and Lett P D 2009 *Nature* **457** 859
[10] Pooser R C, Marino A M, Boyer V, Jones K M and Lett P D 2009 *Phys. Rev. Lett.* **103** 010501
[11] Lawrie B J, Evans P G and Pooser R C 2013 *Phys. Rev. Lett.* **110** 156802
[12] Lawrie B J and Pooser R C 2013 *Opt. Express* **21** 7549
[13] Clark J B, Glasser R T, Glorieux Q, Vogl U, Li T, Jones K M and Lett P D 2014 *Nat. Photonics* **8** 515
[14] Otterstrom N, Pooser R C and Lawrie B J 2014 *Opt. Lett.* **39** 6533
[15] Pooser R C and Lawrie B J 2015 *Optica* **2** 393
[16] Fan W J, Lawrie B J and Pooser R C 2015 *Phys. Rev. A* **92** 053812
[17] Embrey C S, Turnbull M T, Petrov P G and Boyer V 2015 *Phys. Rev. X* **5** 031004
[18] Vogl U, Glasser R T and Lett P D 2012 *Phys. Rev. A* **86** 031806
[19] Vogl U, Glasser R T, Glorieux Q, Clark J B, Corzo N V and Lett P D 2013 *Phys. Rev. A* **87** 010101
[20] Vogl U, Glasser R T, Clark J B, Glorieux Q, Li T, Corzo N V and Lett P D 2014 *New J. Phys.* **16** 013011
[21] Fang Y M, Feng J L, Cao L M, Wang Y X and Jing J T 2016 *Appl. Phys. Lett.* **108** 131106
[22] Jing J T, Liu C J, Zhou Z F, Ou Z Y and Zhang W P 2011 *Appl. Phys. Lett.* **99** 011110
[23] Hudelist F, Kong J, Liu C J, Jing J T, Ou Z Y and Zhang W P 2014 *Nat. Commun.* **5** 3049
[24] Qin Z Z, Cao L M, Wang H L, Marino A M, Zhang W P and Jing J T 2014 *Phys. Rev. Lett.* **113** 023602
[25] Cai Y, Feng J L, Wang H L, Ferrini G, Xu X Y, Jing J T and Treps N 2015 *Phys. Rev. A* **91** 013843
[26] Wang H L, Zheng Z, Wang Y X and Jing J T 2016 *Opt. Express* **24** 23459
[27] Wang H L, Cao L M and Jing J T 2016 *Sci. Rep.* **7** 40410
[28] Coffman V, Kundu J and Wootters W K 2000 *Phys. Rev. A* **61** 052306
[29] Amico L, Fazio R, Osterloh A and Vedral V 2008 *Rev. Mod. Phys.* **80** 517
[30] Rigolin G, Oliveira T R and Oliveira M C 2006 *Phys. Rev. A* **74** 022314
[31] Jasperse M, Turner L D and Scholten R E 2011 *Opt. Express* **19** 3765